

# DETECTING FOREST DEGRADATION IN THE CONGO BASIN BY OPTICAL REMOTE SENSING

Mathieu Rahm<sup>(1)</sup>, Joeri Van Wolvelaer<sup>(1)</sup>, Anton Vrieling<sup>(2)</sup> and Benoit Mertens<sup>(3)</sup>

<sup>(1)</sup> EUROSENSE, 54, Avenue des nerviens, 1780 Wemmel, Belgium, Email: [mathieu.rahm@eurosense.com](mailto:mathieu.rahm@eurosense.com)

<sup>(2)</sup> Faculty of Geo-Information Science and Earth Observation (ITC), University of Twente, P.O. Box 217, 7500 AE Enschede, the Netherlands, Email: [a.vrieling@utwente.nl](mailto:a.vrieling@utwente.nl)

<sup>(3)</sup> Institut de Recherche et Développement (IRD), Maison de la télédétection, 500 rue JF Breton, 34093 Montpellier, France, Email : [benoit.mertens@ird.fr](mailto:benoit.mertens@ird.fr)

## ABSTRACT

Detection of forest degradation with remote sensing remains a challenge. Features of interest are of small spatial size and their spectral reflectance is quickly affected by vegetation regrowth. Tested initially using very high resolution data (QuickBird and WorldView) for two study sites in the Congo Basin, this paper presents the results of a semi-automated object-based method applied using 5-meter resolution RapidEye data for a third study site. In a next step, we applied the same method and compared the classification results based on degraded RapidEye imagery (to 10 and 20m) to evaluate the potential of lower resolution data (such as from the upcoming Sentinel-2) to detect forest degradation in the Congo Basin.

## 1. INTRODUCTION

Deforestation and forest degradation constitute the second largest anthropogenic source of carbon emission in the atmosphere [1]. To mitigate climate change, the United Nations Framework Convention on Climate Change (UNFCCC) has adopted a programme to Reduce Emissions from Deforestation and forest Degradation (REDD+) in developing countries. Implementation of the REDD+ programme should lead to compensations to participant countries if they can prove that adopted policies significantly reduce their carbon emissions as compared to reference levels. Therefore, the development of a robust, reliable and transparent forest monitoring system that allows for credible Measurement, Reporting and Verification (MRV) of REDD+ activities is a crucial element for countries to receive benefits from REDD+. A key component of an MRV system is the monitoring of changes in forest area. Remote sensing is an important component for the development of forest monitoring systems [2]. Through systematic acquisition of satellite imagery, remote sensing provides synoptic overviews that can identify changes in forest cover for larger areas, as compared to ground-based surveys.

While deforestation can be assessed accurately with remote sensing data, detection and mapping of forest

degradation is more challenging [3]. In this case, forest is not replaced by a different land cover, but a change occurs in forest land remaining forest land. Degraded forests are a complex mix of different land cover (vegetation, dead trees, soil, shade) where features of interest are of small spatial size, and vegetation regrowth quickly affects (within a year) their spectral reflectance [2].

To date, there are no widely accepted and operational approaches for direct mapping of forest degradation with remote sensing data. In most studies, medium resolution sensors such as Landsat (30m spatial resolution) have been used for this purpose but many small-size degradation features (such as small-scale non-mechanized logging) cannot be detected at that spatial resolution. Higher-resolution imagery, such as acquired by RapidEye, QuickBird or WorldView, is required to directly map forest canopy damage of these types [2].

Deforestation or forest degradation maps can be derived in two ways from optical high resolution data: through visual interpretation or by computer-based automated procedures. The former has the advantage of using human pattern recognition, which is often superior to automated methods in terms of accuracy [4]. Unfortunately, it is also tediously slow as compared to the processing speed of automated procedures that in addition provide more quantitative and repeatable information [5]. Semi-automated image classification methods are proposed to combine the advantages of both techniques. The most common automated techniques to derive thematic maps from remotely sensed imagery are either pixel-based or object-based. Based on a comparison of both using very high resolution (VHR) imagery, van de Voorde et al. [6] concluded that object-oriented methods are best suited to deal with the complex content of these images. The main drawback of pixel-based methods is the resulting “salt and pepper” effect whereas the object-based method combines the contextual information (i.e., information on surrounding pixels like texture) with spectral information to group similar contiguous pixels into objects [5].

This research aims at developing a methodology to detect, map and quantify deforestation and forest degradation (e.g. forest canopy gaps, small clearings, logging roads) from optical high spatial resolution satellite imagery (<10m). The methodology was first developed for two study sites in the Congo Basin as part of the European Union-funded REDDiness project. We used multispectral VHR data of QuickBird and WorldView-2 (respectively 2.4m and 2m spatial resolution) for a 200-km<sup>2</sup> site in the south of the Republic of Congo, and for a same-sized site in central Gabon, to detect forest degradation. In this paper we report on the application of the method to a third study site in the Democratic Republic of Congo in the framework of the EO4REDD project, financed by the Belgian Walloon region. Within EO4REDD, the same method was tested using RapidEye data (5m spatial resolution). In a next step, we degraded the spatial resolution of the RapidEye imagery (to 10 and 20m) to evaluate if options exist to monitor forest degradation in the Congo Basin with lower-resolution data (for example by the upcoming Sentinel-2).

## 2. STUDY SITES AND DATA

The EO4REDD study site is located 200 km north from Kinshasa in the province of Bandundu, at the western border of the Democratic Republic of Congo (DRC). It is located within the Maï Ndombe integrated REDD+ programme of DRC, which aims to progressively federate a range of initiatives into a coherent REDD+ programme at the district level [7]. The study site covers 15,000 km<sup>2</sup> with predominantly flat topography that is on average 340 m above sea level. The main causes of deforestation and forest degradation in the study area include the development of agricultural activities and the increase of demand for fuel wood and timber from urban population growth.

We acquired a total of 60 RapidEye images with a cloud cover percentage inferior to 20%, i.e., one set of 30 images for July-August 2011, and the other set for July-August 2012. Both datasets were acquired during the same period of the year to reduce possible changes between images that relate to seasonality. In parallel, one pair of QuickBird images (2.4 m spatial resolution) covering 324 km<sup>2</sup> of the study area was ordered for the same period and acquired respectively on 6 September 2011 and 9 January 2013. All acquired images were delivered as orthorectified products by the image providers. This paper focusses on a small-set, covering one RapidEye scene.

Three preprocessing steps were applied to the imagery to allow for an effective comparison. First, all QuickBird and RapidEye images were co-registered to avoid false change detection. Second, each image was radiometrically corrected to obtain top-of-atmosphere (TOA) reflectance using the calibration parameters of

RapidEye and QuickBird. Finally, clouds, haze and shadow areas were systematically removed using multi-threshold object-based segmentation techniques based on the blue band (for cloud/haze detection) and the combination of red-edge and red bands (for shadow detection).

Besides the most widely-used normalized difference vegetation index (NDVI), the Soil Atmospherically Resistant Vegetation Index (SARVI) was calculated and successfully used to identify burned areas. This index further minimizes the atmospheric effects on the NDVI index by engaging the red and blue channels instead of the red one only [8].

## 3. METHODOLOGY

The methodology comprises multi-threshold object-based segmentation techniques where the thresholds set for assigning a class can be adjusted by an operator to combine advantages of automated object-based methods and visual interpretation. This combination of visual and automated methods ascertains high classification accuracy, one of the key requirements of REDD+-MRV systems. The method includes four steps: (1) construction of a forest mask, (2) detection of deforested areas, (3) multi-date segmentation, and (4) detection of degraded areas. The methodology was applied to RapidEye images from 2011 and 2012, hereafter referred to as t0 and t1. Following slight adaptations to thresholds used, the same methodology was applied on the same RapidEye images with a degraded resolution of 10 and 20 m.

### 3.1. Forest mask

A forest mask was made to exclude irrelevant land cover classes and focus the analysis only on forest changes [9]. The use of a mask optimizes the processing time needed in subsequent steps. It also enables the definition of better tailored segmentation rules, which do not need to take into account the complete image heterogeneity, given that the area within the forest mask is far more homogeneous.

The forest mask was realized for the reference image, namely image t0, because we assumed that no forest regeneration occurred between both image acquisitions. Forest was separated from non-forest classes using a multi-threshold segmentation algorithm. The algorithm takes as input two user-defined parameters, i.e., spectral threshold values and minimum object size. The mask creation was performed by consecutive threshold segmentations using different spectral parameters (SARVI, and the green, red edge, and red image bands) to improve the forest mask step by step. The minimum object size was set at 200 pixels to ascertain that the minimum mapping unit (MMU) matches the adopted threshold of forest definition (0.5ha) [10].

Three classes resulted from this first segmentation process: no data, forest and non-forest. No data encompasses clouds, haze and cloud shadows. Forest corresponds to forested areas with a closed canopy. Non-forest includes large clearings and logging roads, roads, built-up areas, agricultural fields, savannah, fallow and water bodies.

### 3.2. Forest change detection

Multi-temporal analysis was carried out to (i) enhance areas where changes occurred and (ii) estimate different levels of forest degradation within multi-date objects.

Areas that were deforested between 2011 and 2012 were delineated within the forest mask of  $t_0$  using the same multi-threshold segmentation function on image  $t_1$ . The minimum object size was again set at 200 pixels to match with the threshold of forest definition.

Subsequently, degradation features ( $<0.5$  ha) were detected in the area that was forest in  $t_0$  and in  $t_1$ , i.e., in the forest that remained forest. These consisted of logging roads and small clearings. The aim of this step was to create a forest degradation map that estimates the level of forest degradation between both dates. The approach is based on multi-date segmentation that uses the image information of multi-date images over the same location to create multi-date objects. Such objects group pixels that are spatially, spectrally and temporally similar [5]. Three parameters need to be defined: scale, colour and shape. The scale parameter determines the size of image objects. If the scale value is high, the variability allowed within each object is high and image objects are relatively large. Conversely, small scale values restrain the variability within each segment, creating relatively smaller objects. The criteria used for colour or shape affect the resulting image object by determining the spectral or spatial homogeneity. Within the shape criterion, the user can also alter the compactness of the object and the smoothness of the objects boundaries.

First, we performed a multi-date segmentation from  $t_0$  and  $t_1$  images to create large multi-date objects, using colour, scale and shape parameters. This first object level (level-1) will be used for the subsequent change detection. The second segmentation level (level-2)

creates small objects within the large level-1 objects using a multi-threshold segmentation technique. This segmentation was applied separately on each image (image  $t_0$  and  $t_1$ ) using the output of level-1 objects to constrain the detection of small patches of forest degradation (canopy gaps and small clearings). The detection of small forest gaps was performed based on the red edge (detection of low vegetation) and near-infrared bands (detection of bare soil). The applied minimum area of created objects was set to 6 pixels (0.015 ha). Finally, five levels (0-5%; 5-20%; 20-50%; 50-70%; 70-100%) of forest degradation are defined for each level-1 object according to the difference of relative area of level-2 objects per level-1 objects between  $t_0$  and  $t_1$ .

### 3.3. Accuracy assessment

Depending on the availability, different data sources may be used to assess the thematic accuracy of the produced maps. While field observations coinciding with the image dates are preferred, also VHR imagery, such as from aerial photograph or possibly Google Earth, could be used. For this case study, we could not obtain sufficient independent reference data through well-timed field campaigns. Moreover, the acquired pair of VHR QuickBird imagery, which was intended for this purpose, could not be used effectively because their acquisition time was delayed compared to RapidEye. QuickBird imagery was acquired on 6 September 2011 and 9 January 2013, whereas RapidEye imagery over the same location was acquired on 20 July 2011 and 25 August 2012. Even within the relatively short 1.5 months interval between 20 July and 6 September 2011, many changes could be observed (Fig. 1). For that reason we decided to use the RapidEye imagery both for classification and accuracy assessment.

The thematic accuracy of the forest maps was assessed via a stratified random sampling strategy. The amount of validation points in each land cover class (forest, non-forest, deforested and degraded areas) was selected based on the area covered by the class. For each land cover classification, an error matrix was computed in which three accuracy indices were derived: the overall accuracy and, the omission and commission error.

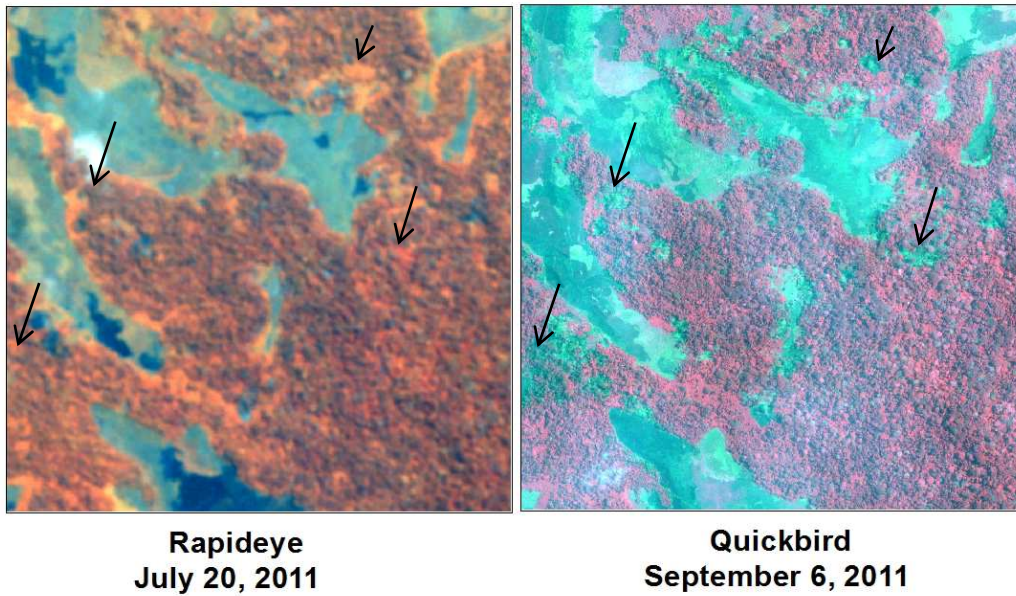


Figure 1: Land cover changes between QuickBird and RapidEye data acquired at 1.5 months interval. Arrows show some change locations.

#### 4. RESULTS

##### 4.1. Degradation map

Areas that were deforested or degraded between 2011 and 2012 were identified for one pair of RapidEye images. The generalized change map simplified at coarser scale (level-1 multi-date large objects) with five levels of forest degradation is shown in Fig. 2. Deforested areas, which correspond to a degradation level of 100%, are represented with forest degradation level 5 classes (70-100%). The object detection of deforested and degraded areas (small forest gaps, logging roads) is presented in Fig. 3 over an image subset.

From a forest extent of 34,233 ha on the RapidEye image of 2011, about 388 ha were deforested and 267 ha were degraded in August 2012.

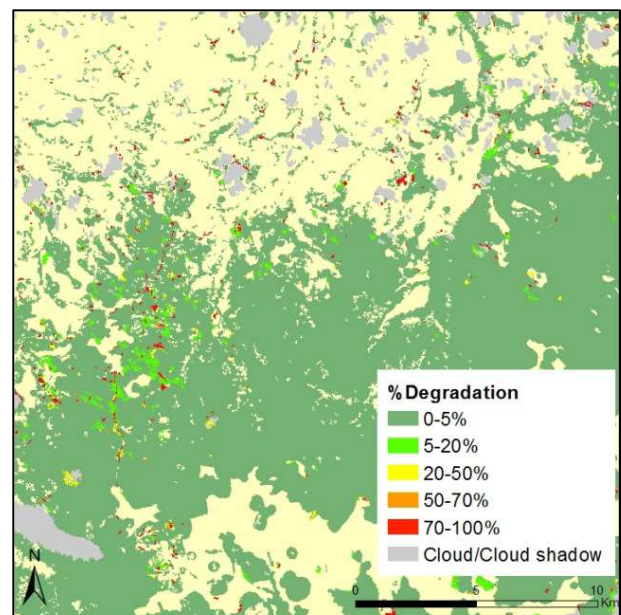


Figure 2: Generalized forest degradation map over a subset of the study area

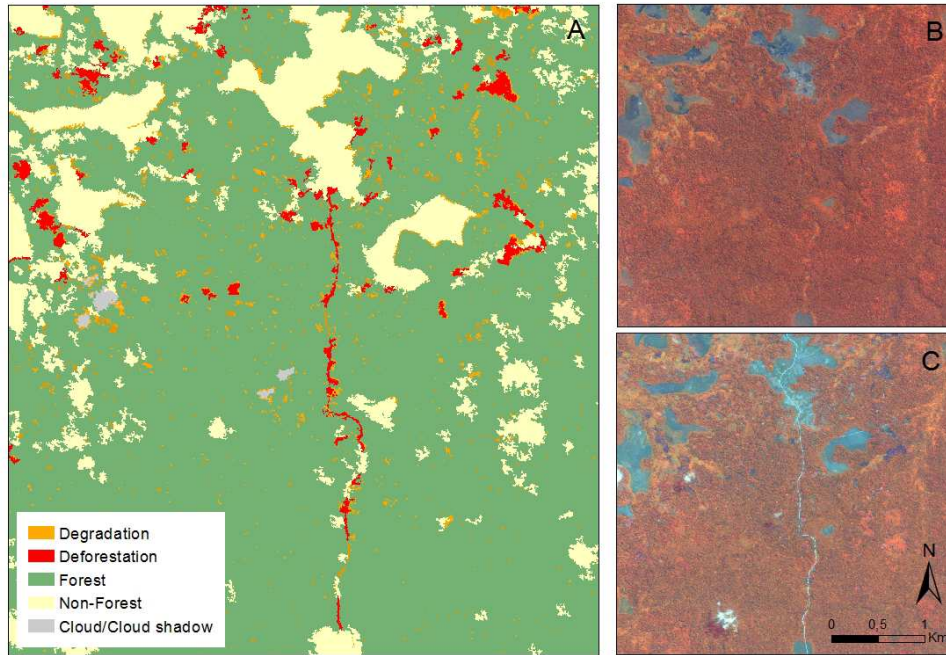


Figure 3: RapidEye image subset: A) overlaid by the detected deforested and degraded areas in August 25, 2012, B) from July 20, 2011 and C) from August 25, 2012

#### 4.2. Results comparison using different resolution data

For a better understanding of the potential of current and future optical high resolution data to detect forest degradation in the Congo Basin, the exact same steps of the methodology were applied to RapidEye data degraded to 10 and 20 m resolution. Given the modification of the image parameters, the threshold for spectral and minimum object size (number of pixels) of the multi-threshold segmentations were adapted to enhance the detection of forested, deforested and degraded areas. In order to better match with the minimum mapping unit of the classification based on the RapidEye image at 5m (0.015 ha), the minimum object size for the detection of degraded areas based on RapidEye at 10 and 20m was set to 2 pixels (0.02 ha) and 1 pixel (0.04 ha), respectively. Fig. 4 shows a comparison of the differences in the detection of deforested and degraded areas based on spatial resolution.

When comparing the results of the three classifications, it appeared that the extent of deforested areas was increasingly overestimated when coarsening the image, i.e., 388 ha for 5m, 425 ha for 10m, and 407 ha for 20m resolution. This situation was reversed for

degraded areas, i.e., 267 ha for 5m, 209 ha for 10m, and 173 ha for 20m resolution.

Tab. 1 shows the accuracy assessment results of the deforestation and forest degradation mapping method based on RapidEye data at 5, 10 and 20 m. Results are presented for the two steps of the methodology, namely the forest mask (forest/non-forest classification) and the change detection. The semi-automated forest mask and the change detection classifications based on data at 5 m achieved an overall accuracy of 99.2% and 91.5% respectively. Errors were due to omissions (0.7 and 5.7%) but mainly to commission errors (1.1 and 12.5%). The overall accuracy of both classifications decreased when using data at lower resolution, while omission and commission errors were increased. Given that the minimum mapping unit increased with the use of data at lower resolution, a higher percentage of omission errors was expected. Nevertheless, even when applied to degraded RapidEye data, the method showed high accuracy (>88%) and good detection of forest degradation.

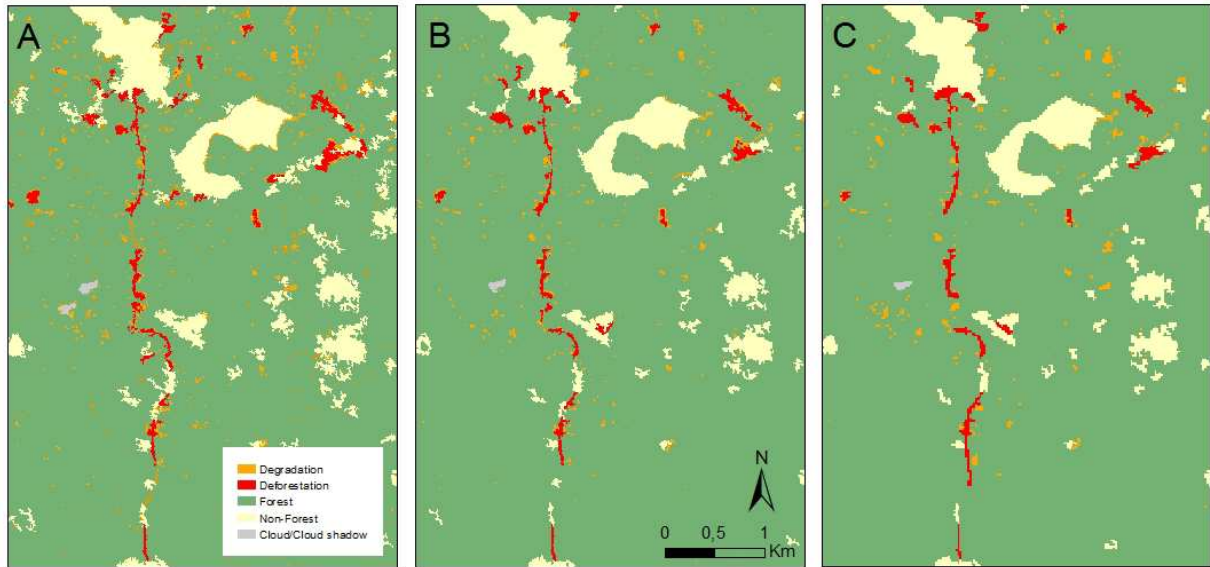


Figure 4: Detected deforested and degraded areas between 20 July 2011 and in 25 August 2012 based on RapidEye data A) at 5 m B) degraded at 10 m and C) degraded at 20 m resolution.

Table 1. Accuracy assessment results (n=118) for the two steps of the deforestation and forest degradation mapping method, namely the forest/non-forest (F/NF) when using RapidEye data at 5, 10 and 20 m

	F/NF classif. (5 m)	Change detection (5 m)	F/NF classif. (10 m)	Change detection (10 m)	F/NF classif. (20 m)	Change detection (20 m)
Overall accuracy (%)	99.2	91.5	95.8	89.7	94.1	88.9
Omissions (%)	0.7	5.7	8.7	10.2	13.3	11.8
Commissions (%)	1.1	12.5	9.5	13.5	12.4	14.5

## 5. DISCUSSION AND CONCLUSIONS

The object-based change detection method proposed in this study proved to be an efficient and accurate approach to detect, map and quantify deforestation and forest degradation over fragmented landscapes in the Congo Basin. The object-based method combines the advantage of the contextual analysis of visual interpretation with the quantitative spectral information, and as such is an important asset when classifying the complex mix of different land cover in degraded areas. The operator can proceed step by step through the classification process and adjust the thresholds set for assigning a class in order to enhance the classification accuracy. Moreover, the method proved to be replicable since it was successfully applied to different study areas with various sensors and image resolutions. However, extension of this promising method to the whole study area (15,000 square kilometers) still provides challenges. Given that the semi-automated method is based on the use of optical sensors, thresholds set for assigning classes often need to be adjusted to reduce misclassifications resulting from radiometric distortions and atmospheric

effects that are different among scenes. Moreover, when forest types, or drivers of forest degradation change, degradation features may become less discernible from the imagery [3].

The method proposes two levels of analysis to evaluate forest degradation. Level-1 multi-date objects aggregate information about small degradation features over larger area to highlight five levels of forest degradation, whereas smaller level-2 objects show the extent and the exact location of these small features. The forest degradation map gives an overview at coarser scale of the location and the intensity of degraded areas in the study area. This provides useful information for understanding the phenomenon and drivers of forest degradation. Within the study area, most of degraded areas are located near human settlements and along the reopened road. Drivers of forest degradation are mainly related to shifting cultivation and logging activities.

Despite the overall success in the exercise reported on here, limitations remain for monitoring forest degradation features by optical remote sensing.

Vegetation regrowth rapidly reduces the detection of small features related to degradation, as we could observe from imagery separated by only 6 weeks (Fig. 1). Therefore, good-quality cloud-free remote sensing imagery needs to be acquired at frequent intervals (at least once per year). This limits the use of optical data especially in cloudy regions such as the study area. For instance, archives of VHR data are very limited and new image acquisition with limited cloud cover is often delayed. Moreover, the added high cost and small ground swath of this type of data hinder its use to monitor large areas. However, the results of this study show that data from high resolution sensors (<20 m) have potential for detecting forest degradation with good accuracy (>88%). This type of data which has higher ground swath, higher revisiting frequency capabilities, and lower cost seems to be best suited for monitoring forest degradation over large areas. In this study, RapidEye showed efficient acquisition capabilities of good-quality data. Two datasets of wall-to-wall image mosaic at 5 m resolution were acquired at one year interval (July 2011 and August 2012) with limited cloud cover for the study area spanning 15,000 square kilometers in DRC. Moreover, the presence of a red edge band sensitive to chlorophyll status and canopy structure improved the detection between low vegetation and forest. The near future launch of Sentinel-2, which combines a large swath (290 km), frequent revisit, and systematic acquisition of all land surfaces at high-spatial resolution with a large number of spectral bands (including the red edge) [11], is very promising for future monitoring of forest degradation. Moreover, Sentinel-2 is promised to have an open data policy, which would greatly enhance the future setting up of cost-effective operational services for degradation monitoring.

## 6. ACKNOWLEDGEMENT

This research has been funded by the Belgian Walloon region and the European Union in the framework of two related projects, respectively EO4REDD and REDDiness.

## 7. REFERENCES

1. van der Werf, G. R., Morton, D. C., Defries, R. S., Olivier, J. G. J., Kasibhatla, P. S., Jackson, R. B., Collatz, G. J., Randerson, J. T. (2009). CO<sub>2</sub> emissions from forest loss. *Nature Geoscience*, Volume 2, Issue 11, pp. 737-738.
2. GOF-C-GOLD. (2012). A sourcebook of methods and procedures for monitoring and reporting anthropogenic greenhouse gas emissions and removals associated with deforestation, gains and losses of carbon stocks in forests remaining forests, and forestation. GOF-C-GOLD Report version COP18-1, GOF-C-GOLD Land Cover Project Office, Wageningen University, The Netherlands.
3. Herold, M., Román-Cuesta, R. M., Mollicone, D., Hirata, Y., Van Laake, P., Asner, G. P., Souza, C., et al. (2011). Options for monitoring and estimating historical carbon emissions from forest degradation in the context of REDD+. *Carbon balance and management*, 6(13), 1–7.
4. Duveiller G, Defourny P, Desclée B, Mayaux P. (2008), Deforestation in Central Africa: estimates at regional, national and landscape levels by advanced processing of systematically-distributed Landsat extracts. *Remote Sensing of Environment* 112, 1969–1981
5. Desclee, B., P. Bogaert & P. Defourny (2006) Forest change detection by statistical object-based method. *Remote Sensing of Environment*, 102, 1-11.
6. Van de Voorde, T., De Genst W., Canters F., Stephenne N., Wolff E., Binard M. (2004). Extraction of Land Use / Land Cover - Related Information from Very High Resolution Data in Urban and Suburban Areas. In *Proc. 23th Symposium of the European Association of Remote Sensing Laboratories* (Ed. R. Goossens), Ghent, Belgium, pp 237-244
7. Ministère de l'Environnement, Conservation de la Nature et Tourisme Coordination Nationale REDD. (2010). Programme intégré REDD+ à l'échelle du District de Mai Ndombe, document d'orientation. Online at: [http://www.redd.cd/sites/default/files/documents/prog\\_redd\\_rdc\\_note\\_orientation\\_district\\_de\\_mai\\_ndombe.pdf](http://www.redd.cd/sites/default/files/documents/prog_redd_rdc_note_orientation_district_de_mai_ndombe.pdf) (as of 6 September 2013)
8. Kaufman, Y.J. and Tanre. D. (1992). Atmospherically resistant vegetation index (ARVI) for EOS-MODIS. *IEEE Transactions on Geoscience and Remote Sensing* 32 (2): 261-270.
9. Coppin, P.R. and Bauer, M.E. (1996). Digital change detection in forest ecosystems with remote sensing imagery. *Remote Sensing Reviews* 13:207-234.
10. FAO. (2010). Global Forest Resources Assessment 2010. Main report. FAO Forestry Paper No. 163. Rome.
11. Drusch, M., Del Bello, U., Carlier, S., Colin, O., Fernandez, V., Gascon, F., et al. (2012). Sentinel-2: ESA's Optical High-Resolution Mission for GMES Operational Services. *Remote Sensing of Environment*, 120, 25–36.